Rhythmic Growth Combined with Lamellar Twisting Induces Poly(ethylene adipate) Nested Ring-Banded Structures

Yiguo Li,[†,‡] Haiying Huang,[†,‡] Tianbai He,*[,†,‡] and Zongbao Wang*[,§]

[†]State Key Laboratory of Polymer Physics and Chemistry, Changchun Institute of Applied Chemistry, Chinese Academy of Sciences, Changchun 130022, P. R. China

[‡]Graduate School of the Chinese Academy of Sciences, Beijing 100049, P. R. China

[§]Ningbo Key Laboratory of Polymer Materials, Ningbo Institute of Material Technology and Engineering, Chinese Academy of Sciences, Ningbo, 315201, P. R. China

ABSTRACT: Previously, poly(ε-caprolactone) (PCL) classical ring-banded spherulites with periodic twisted lamellae and nonclassical concentric ringed structures induced by rhythmic growth were obtained by modulating the competition between diffusion flux and spherulitic growth. In this study, the modulation of diffusion flux and spherulitic growth on ring-banded structures is further studied, and hierarchical nested ring-banded patterns with a banded structure nested in the ridge rings of the other concentric ringed structure are prepared during slow solvent evaporation in poly(ethylene adipate) (PEA) solution films. The structural characterizations reveal that the big concentric ringed structure derives from periodic variation of thicknesses and that the small inner banded structure consists of periodic twisted lamellae. A diffusion-induced rhythmic growth mechanism and an unbalanced surface stress induced lamellar twisting model are proposed to illustrate the formation of the big concentric and the inner banded structures, respectively.

anded (or ringed) morphology is frequently observed in polymer spherulites. The formation mechanism of this morphology has been widely investigated in the past decades but still remains controversial.[1,2] In the most accepted explanation, the appearance of bands is proposed as a result of periodic twisting of ribbon-like lamellae along the radial growth direction of the spherulites,[1−5] and Keith and Padden[3] ascribed the twisting of lamellae to the unbalanced stresses at the opposite fold surfaces caused by the significantly different overcrowding and inefficient packing in fast-growing lamellar crystals. The periodic continual twisting of lamellar crystals in banded spherulites have been confirmed by microscopic observations for poly(trimethylene teraphthalate)[6,7] and its copolymers with poly(lactic acid),[7] poly(3-hydroxybutyrate-co-hydroxyhexanoate),[8] and poly(3-hydroxybutyrate-co-hydroxy-valerate) (PHBV).[9] Lotz and Cheng extensively studied the origin of lamellar twisting in a comprehensive review, and they believed that the difference in surface stresses from structural features was the origin for the twisting of lamellae.[10] However, Kyu et al.[11,12] who, based on experimental results of polymer blends[11] and the corresponding simulation,[12] suggested that the twisting of lamellae might not be the only reason for the formation of banded structures, that the concentric ringed structures might be a consequence of rhythmic crystal growth resulting from nonlinear diffusion during growth. Indeed, Chen et al.[13,14] observed ringed features in blends of aromatic poly(ether ketone)s without lamellar twisting. Notably, Duan et al.[15,16] and Wang et al.[17] reported rhythmic growth-induced concentric ringed structures consisting of multilayer flat-on lamellar crystals in isotactic polystyrene and poly(bisphenol A

hexane ether) (BA-C6) thin films, respectively. In our previous work,[18,19] by controlling the evaporation of solvent at a slow rate during solution crystallization, poly(ε-caprolactone) (PCL) concentric ringed structures with a periodic variation of thickness were obtained. The nonclassical banded structures were confirmed to be owing to the competition between diffusion flux of polymer chains in solution, J, and spherulitic growth with the radial growth velocity, V. Furthermore, by modulating the interplay between J and V, classical PCL banded spherulites consisting of periodic twisted lamellae were successfully prepared using the same method when J decreased and V increased to dominance.[20] Kyu et al.[12] have reckoned a reconciliation between the lamellar twisting model and the rhythmic growth model based on theoretical simulation. There may be no absolutely reconciliation between the two models, but it is reasonable to expect that the two models coexist at suitable conditions. Motivated by such idea, therefore, in the present paper, our research will focus on exploring the two banded patterns generated in one spherulite by controlling the preparation conditions and the related competition between J and V.

In this letter, poly(ethylene adipate) (PEA) was chosen because its lamellar crystals are expected easily twist from structural features, and it is suitable for the method used previously. A novel hierarchical nested ring-banded pattern, in which one kind of banded structure is nested in the ridge rings
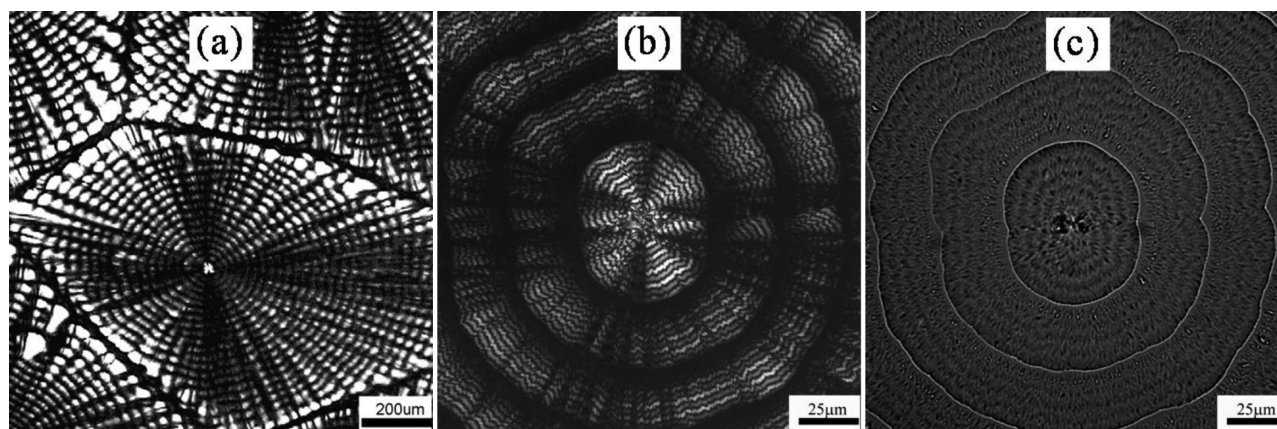
Figure 1. (a) Polarized optical micrograph of the typical PEA nested ring-banded structures and magnified micrographs of the nested ring-banded structures obtained under (b) crossed-polarized and (c) unpolarized light.

of the other concentric ringed structure, was prepared by controlling the solvent evaporation procedure from PEA solution films. The observation of PEA nested ring-banded structures may provide the first piece of direct experiential evidence for the coexistence of the lamellar twisting model and the rhythmic growth model.

By controlling the solvent evaporation rate during solution casting, a novel PEA ring-banded structure was achieved from a 5 mg mL^{-1} solution of PEA in tetrahydrofuran (THF) at a slow solvent evaporation rate of 4.2×10^{-4} mL h^{-1} at 20 °C. Fine regularly concentric ringed patterns with alternating bright and dark rings, as well as the Maltese cross are observable under crossed-polarized light (Figure 1a). However, unlike classical banded spherulites in which the widths of the bright and dark bands are approximately equal, the bright rings are much wider than the dark ones in these spherulites. A higher magnification POM image shows that there are several small bands nested in the bright rings of the structures (Figure 1b). Furthermore, these small bands are typical double-banded features which have narrow extinction black lines between alternating bright and dark bands. The striking patterns are also discernible under unpolarized light (Figure 1c). It is apparent that the big concentric ringed structures exhibit sharp contrast under both polarized and unpolarized light, while the small banded patterns, similar to classical banded spherulites, show sharp contrast under polarized light but poor contrast under unpolarized light. The ring-banded structures are clearly different from classical PEA banded spherulites which only have double-banded patterns[21−24] and are also distinct from PCL concentric ringed structures with a periodic variation of thickness.[18,19] Now, it is obvious that there are two different kinds of ringed or banded structures in a single spherulite. To distinguish them, we defined the concentric rings as "big rings" and the double-bands nested in the "big bright rings" as "inner bands", so the whole spherulites are named "nested ring-banded spherulites". The sizes of the nested ring-banded spherulites are 0.5−5 mm, and the periodicities of the big rings and inner bands were measured to be 24.0 and 5.5 μm, respectively. Another interesting feature is the regular waviness along the circumference of each big ring, which can be attributed to the thickness difference along tangential direction resulting from the preferred growth of some lamellae and the concomitant lateral depletion of materials. It should be mentioned that the thickness difference between the interior and the edge of the film is slight in this case and that the nested

ring-banded nature of the crystals is independent of thickness within this range.

It is known that the appearance of double-banded patterns is a consequence of a biaxial indicatrix twisting about the optical normal.[24,25] They have also been observed in a number of other polyesters, like poly(3-hydroxybutyrate),[26] poly(ethylene sebacate) (PES),[27,28] and PHBV.[29] PEA is known to crystallize only in monoclinic structure, and according to its biaxial optical character with dissimilar principal refractive indices ($n_3 > n_2 > n_1$),[30] double-banded patterns are expected when the lamellae are twisted along the a*-axis. All features of the inner bands are the same as those of the PEA double-banded spherulites formed from melt crystallization.[20−23] Therefore, it is concluded that the inner banded structures in big ridge bands are owing to lamellar twisting about the optical normal.

To further investigate the PEA nested ring-banded structures, atomic force microscopy (AFM) was applied to characterize the novel morphology. The striking morphology can be seen both in AFM height (Figure 2a) and phase photographs (Figure 2b). Therein, the height image gives clearer big rings, while the phase image exhibits more distinct inner bands. Both the three-dimensional height image (Figure 2c) and height profile along the added line indicated in height image (Figure 2d) show that the big ringed structures consisted of alternating ridge and valley rings with a periodic variation of thickness. The ridge-to-valley height difference, 1100−1300 nm, is close to the average thickness of film, ca. 1000 nm, which confirms that the big rings are resulting from the periodic variation of thickness. Furthermore, unlike the rhythmic growth-induced PCL concentric ringed structures that exhibit smooth height profile,[18,19] the height profile of PEA nested ring-banded structures in the thickening process exhibits a relatively complex curve. To reveal the detailed information of the growth process of the nested-banded structures, the higher magnification height profile of a big ring period was represented in Figure 2e (solid line). The height gradual increase and flight undulation are both evidently visible, and the four small peaks correspond to the inner bright bands in AFM height image. Note that the periodic lamellar twisting can induce slight periodic height undulation along the radial direction, which has been displayed by AFM in many polymer banded spherulites.[8,23,31] Considering the ridge-to-valley height difference of classical PEA double-banded spherulites, we obtained the "absolute" height profile (dashed line in Figure 2e) by subtracting the fluctuated height due to lamellar twisting
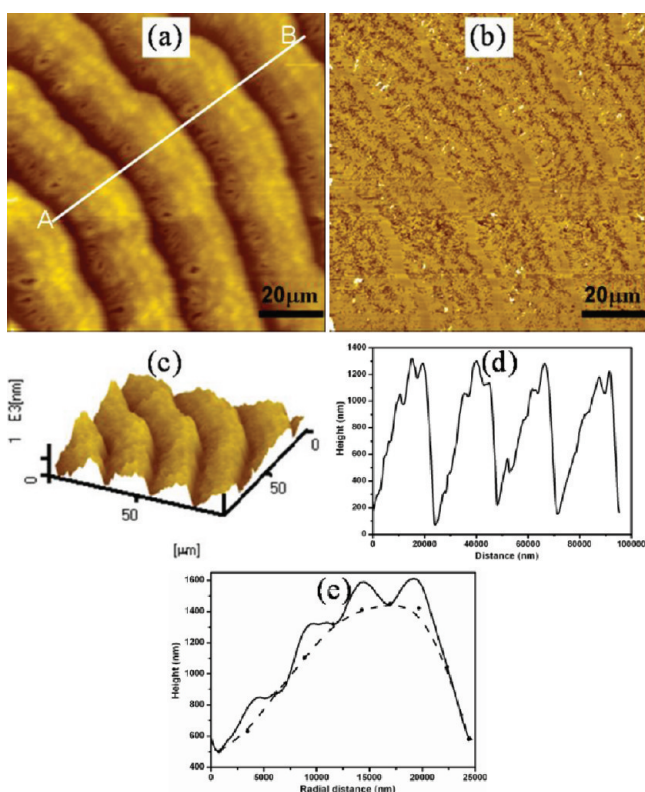
Figure 2. AFM (a) height, (b) phase, and (c) three-dimensional images of PEA nested ring-banded structures. (d) Cross-sectional height profile along the white line added in part a. (e) AFM height profile of a big ringed period of the nested ring-banded structure. The dashed line represents the absolute height profile of the big ringed structures after removing the thickness fluctuation due to lamellar twisting.
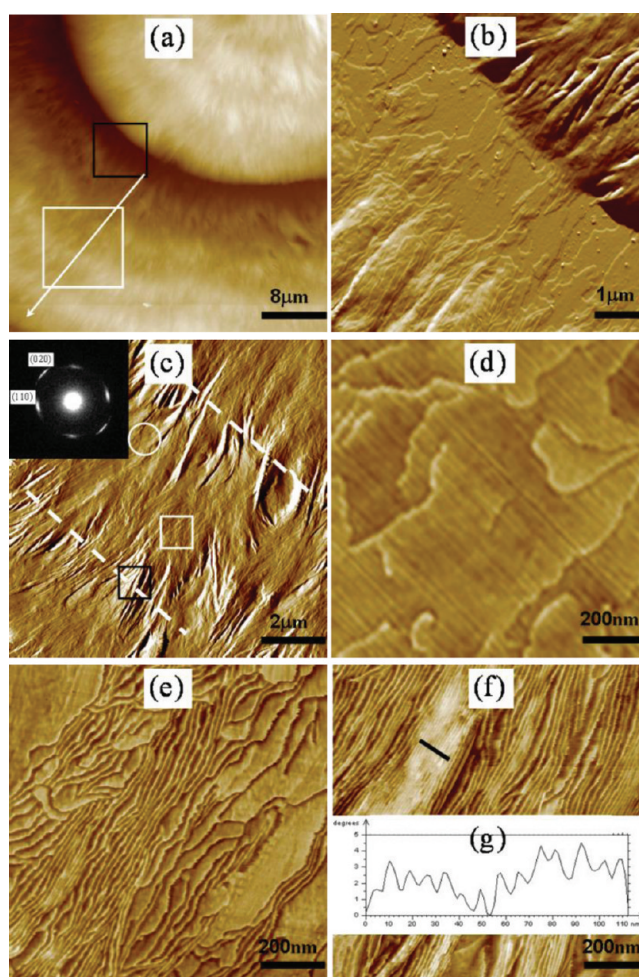

Figure 3. (a) AFM height image of PEA nested ring-banded structures; the white arrow reflects the radial direction. Magnified AFM amplitude images of (b) the big valley ring and (c) the big ridge ring, indicated by black and white square in part a, respectively. The inset in part c is the selected-area electron diffraction pattern of the inner valley (dark) band in the location shown by the white circle. Parts d, e, and f are the phase images of the valley band, transition zone, and ridge band of the inner banded structures, respectively. (g) Cross-sectional phase profile along the black line in part f.

from the original height profile. The "absolute" height profile is quite similar to the height profile of PCL ringed structures with periodic variation of thickness.[18,19] Hence, the height profile of the nested ring-banded structures can be considered as a combination of the height profile of ringed structures with a periodic variation of thickness with the height fluctuation owing to periodic lamellar twisting, which suggests that the nested ring-banded structures may be a combination of the two banded structures.

The morphology and microstructure of PEA nested ring-banded structures were further analyzed by AFM and transmission electron microscopy (TEM) in great detail. Figure 3a illustrates the overall morphology, and Figure 3b,c shows the amplitude images of the valley and ridge rings of the big ringed structures, respectively. It is evident from Figure 3b that the big valley ring is consisted of flat-on lamellar crystals. Meanwhile, in the big ridge rings, the smaller alternating convex and concave inner bands consisting of periodic twisted lamellae can be discriminated in Figure 3c (the ridges are indicated by the broken lines). As revealed in Figure 3d, the inner concave bands are composed of flat-on lamellae. This point is further confirmed by the electron diffraction pattern inset in Figure 3c. All of the diffraction spots can be indexed on the basic of monoclinic unit cell, with parameters a = 0.547 nm, b = 0.732 nm, c = 1.172 nm, and β = 113.5°, of the PEA crystal.[30] Moreover, the (020) diffraction pattern according with the tangential direction of the spherulite reflects that the crystallographic a^*-axis coincides with the radial direction. Figure 3e

shows the tilted lamellar morphology of the transform zone in the location indicated by the white square in Figure 3c. As is illustrated in Figure 3f, more tilted and edge-on lamellar crystals are located at the inner convex band. The cross-sectional phase profile (Figure 3g) along the black line in Figure 3f shows that the average thickness of lamellar crystals is ca. 8 nm. From the results mentioned above, it can be clearly illustrated that the lamellar orientation of the inner bands varies periodically from flat-on, through tilted then to edge-on. The formation of alternating flat-on-to-edge-on morphology in AFM is in accordance with the appearance of alternating dark-to-bright rings under cross-polarized light.[23] It is worthy that all above results about big rings are the same as those of PCL concentric ringed structures with a periodic changing of thickness and the characteristics associating with inner bands are in agreement with those of classical PEA double-banded spherulites obtained from melted crystallization. Therefore, it is concluded that the big rings are derived from the periodic variation of the thickness, and the inner bands result from the lamellar twisting.

In analogy to the development of PCL concentric ringed structures with a periodic variation of thickness, the formation of the big-ringed structures can also be described by a diffusion-induced rhythmic growth associated with periodic changes in the concentration gradient.[18,19] When solvent evaporation caused solution concentrated to the threshold concentration, nucleation occurred. The crystal growth consumed the polymer chains in the advancing front, so that the surrounded material diffuses to feed further crystal growth. As the process proceeds, the length l that polymer needs diffused to the crystal front becomes larger and larger, and thus less and less material can be transported to the growth face. As a consequence, the crystal height gradually decreases; eventually, chains can only supply the very few lamellae for continual growth, and thus the first valley formed. As the valley further proceeds, less chains are consumed, and then a shorter and shorter length is needed to travel, so that more and more chains can be transported to growth front, which induced the increase again in crystal thickness. Hence, the ridge rings resulted. The repetition of this behavior caused the emergence of the big concentric ringed structures. The concentration gradient, G, results from the solution concentration difference between the concentration in growth front, ϕ_{gf}, and the concentration of whole bulk solution, ϕ_{bs}. The changing of diffusion length results from the periodic variation of concentration gradient, $G = (\phi_{bs} - \phi_{gf})/l$, which gives rise to a periodic supply of polymer chains and then results in the rhythmic growth of the crystals. The growth of big concentric rings reflects the competition between the growth of crystals and the diffusion of polymer chains. The formation of alternating ridge and valley rings is owing to that the diffused polymer chains are enough for the ridge rings and insufficient for the valley rings. The twisting of lamellae in the inner bands can be attributed to the unbalanced surface stresses from structural features. Since PCL crystals belong to an orthorhombic system, the twisting of PCL lamellae is difficult, especially in the short distance of one band spacing,[19] which corresponds to the experimental result that PCL ring-banded spherulites are difficult to obtain from melt crystallization. While PEA is known to crystallize only in a monoclinic structure, it is obvious that the chain is tilted in the PEA crystals (which is similar to PES[26,27]). Chain tilt will easily result in different fold encumbrance at opposite fold surfaces of the lamellae and will lead to a difference in the degree of congestion and hence in the magnitude of compressive stresses originating a bending moment responsible for the twisting of lamellar crystals. The development of the nested ring-banded structures can be explained successfully by combining the rhythmic growth mechanism with the lamellar twisting model, as shown in Figure 4. The detail growth insights of the nested
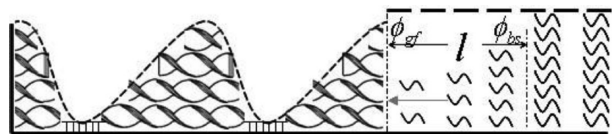

Figure 4. Schematic illustration interpreting the formation mechanism for PEA nested ring-banded structures. The dashed curve on the left of cartoon represents the profile of the big rings, and the dashed line above the diffusion and bulk solution zone indicates the solution surface.

banded structures will be present in a later paper where the growth processes are followed by in situ optical observation,

and the modulation of diffusion flux and spherulitic growth on the nested ring-banded spherulites will be further studied.

In summary, we have obtained a novel hierarchical nested ring-banded structure via controlling the solvent evaporation rate in PEA solution. The big concentric ringed structure with a periodic variation of thickness is resulted from diffusion-induced rhythmic growth, and the inner banded structure with twisted lamellae is due to unbalanced surface stresses from structural features. The unique hierarchical nested ring-banded structures, on one hand, richen crystal morphologies of semicrystalline polymers but, on the other hand, might offer a new perspective to study polymer-banded structures. To further study the modulation of diffusion flux and spherulitic growth on the ring-banded structures, the investigation of ring-banded structures of poly(ϵ-caprolactone)-*block*-poly(ethylene oxide) (PCL-*b*-PEO) copolymer with different topological structures and chain lengths is in progress.

■ EXPERIMENTAL METHODS

Poly(ethylene adipate) was purchased from Aldrich Chemical Co. The weight average molecular weight (M_w) was measured to be 10 000 g mol^{-1} by gel permeation chromatography (GPC). Differential scanning calorimetric measurement indicated the melting point (T_m) of PEA was 47 °C.

The preparation of the PEA nested ring-banded architectures was carried out in PEA/THF solution films by controlling slow solvent evaporation. Before use, the solution was heated to 50 °C for 30 min to dissolve any crystals that might form when the solution was kept for long time at room conditions. A 10 μL solution was cast, at 20 °C, onto precleaned glass slides placed on a stage lodged inside a cylindrical container with a radius and height 1.0 and 2.5 cm, respectively. The container was covered with its lid as soon as the casting finished. Thus, solvent vapor can only escape through the small gap between the container and its lid. A controllable solvent evaporation rate was achieved by adding different amounts of extra THF solvent inside the cylindrical container before casting solution onto the substrate. The PEA nested ring-banded structures were produced at 20 °C under a slow solvent evaporation rate of 4.2×10^{-4} mL h^{-1}, which was achieved by adding 200 μL of extra THF solvent to the container before casting. As the solvent evaporation proceeds, solution first concentrates and then becomes saturated, and eventually the crystallization of PEA takes place. The whole drying process was completed after ca. 24 h.

Polarized optical microscopy (POM) experiments were carried out using a Carl Zeiss A1m microscope equipped with a charge-coupled device (CCD) camera, and transmittance mode was used to obtain the optical images. AFM measurements were performed on SPA-300HV AFM equipped with a SPI 3800N controller (Seiko Instruments Industry Co., Ltd.), and an atomic force microscope (PICOSCAN SPM, Molecular Imaging Inc., now Agilent 5500AFM/SPM System (Agilent Technologies)) was also used. All images were taken with the tapping mode at ambient temperature. For SPA-300HV AFM, the images were collected with a silicon cantilever having a spring constant of 3 N m^{-1} and with a scanning rate of 1 Hz. Meanwhile for the Agilent 5500AFM/SPM system, typical values for the set point were 3−6, and scanning rates ranged from 0.2 to 1 Hz. TEM observation and selected-area electron diffraction (SAED) were conducted by a JEOL JEM-1011 working at an accelerating voltage of 100 kV.

■ AUTHOR INFORMATION

Corresponding Author
*E-mail: tbhe@ciac.jl.cn (T.H.); wangzb@nimte.ac.cn (Z.W.).

Notes
The authors declare no competing financial interest.

ACKNOWLEDGMENTS

REFERENCES

(1) Keith, H. D.; Padden, F. J. *Macromolecules* **1996**, *29*, 7776−7786.
(2) Keith, H. D. *Polymer* **2001**, *42*, 9987−9993.
(3) Keith, H. D.; Padden, F. J. *Polymer* **1984**, *25*, 28−42.
(4) Keith, H. D.; Chen, W. Y. *Polymer* **2002**, *43*, 6263−6272.
(5) Keith, H. D.; Padden, F. J.; Lotz, B.; Wittmann, J. C. *Macromolecules* **1989**, *22*, 2230−2238.
(6) Ho, R. M.; Ke, K. Z.; Chen, M. *Macromolecules* **2000**, *33*, 7529−7537.
(7) Li, J.; Li, Y.; Zhou, J.; Yang, J.; Jiang, Z.; Chen, P.; Wang, Y.; Gu, Q.; Wang, Z. *Macromolecules* **2011**, *44*, 2918−2925.
(8) Xu, J.; Guo, B. H.; Zhang, Z. M.; Zhou, J. J.; Jiang, Y.; Yan, S.; Li, L.; Wu, Q.; Chen, G. Q.; Schultz, J. M. *Macromolecules* **2004**, *37*, 4118−4123.
(9) Wang, Z.; Li, Y.; Yang, J.; Gou, Q.; Wu, Y.; Wu, X.; Liu, P.; Gu, Q. *Macromolecules* **2010**, *43*, 4441−4444.
(10) Lotz, B.; Cheng, S. Z. D. *Polymer* **2005**, *46*, 577−610.
(11) Okabe, Y.; Kyu, T.; Saito, H.; Inoue, T. *Macromolecules* **1998**, *31*, 5823−5829.
(12) Kyu, T.; Chiu, H. W.; Guenthner, A. J.; Okabe, Y.; Saito, H.; Inoue, T. *Phys. Rev. Lett.* **1999**, *83*, 2749−2752.
(13) Chen, J.; Yang, D. C. *Macromolecules* **2005**, *38*, 3371−3379.
(14) Chen, J.; Yang, D. C. *Macromol. Rapid Commun.* **2004**, *25*, 1425−1428.
(15) Duan, Y. X.; Jiang, Y.; Jiang, S. D.; Li, L.; Yan, S. K.; Schultz, J. M. *Macromolecules* **2004**, *37*, 9283−9286.
(16) Duan, Y. X.; Zhang, Y.; Yan, S. K.; Schultz, J. A. *Polymer* **2005**, *46*, 9015−9021.
(17) Wang, Y.; Chan, C. M.; Li, L.; Ng, K. M. *Langmuir* **2006**, *22*, 7384−7390.
(18) Wang, Z. B.; Alfonso, G. C.; Hu, Z. J.; Zhang, J. D.; He, T. B. *Macromolecules* **2008**, *41*, 7584−7595.
(19) Wang, Z. B.; Hu, Z. J.; Chen, Y. Z.; Gong, Y. M.; Huang, H. Y.; He, T. B. *Macromolecules* **2007**, *40*, 4381−4385.
(20) Li, Y. G.; Wang, Z. B.; Hu, Z. J.; He, T. B. Unpublished results.
(21) Takayanagi, M.; Yamashita, T. *J. Polym. Sci.* **1956**, *22*, 552−555.
(22) Woo, E. M.; Wu, P. L.; Wu, M. C.; Yan, K. C. *Macromol. Chem. Phys.* **2006**, *207*, 2232−2243.
(23) Wang, T. C.; Wang, H. J.; Li, H. H.; Gan, Z. H.; Yan, S. K. *Phys. Chem. Chem. Phys.* **2009**, *11*, 1619−1627.
(24) Keith, H. D.; Padden, F. J. *J. Polym. Sci.* **1959**, *39*, 123−138.
(25) Keith, H. D.; Padden, F. J. *J. Polym. Sci.* **1959**, *39*, 101−122.
(26) Ye, H. M.; Xu, J.; Guo, B. H.; Iwata, T. *Macromolecules* **2009**, *42*, 694−701.
(27) Keith, H. D. *Macromolecules* **1982**, *15*, 122−126.
(28) Keith, H. D. *Macromolecules* **1982**, *15*, 114−122.
(29) Jiang, Y.; Zhou, J. J.; Li, L.; Xu, J.; Guo, B. H.; Zhang, Z. M.; Wu, Q.; Chen, G. Q.; Weng, L. T.; Cheung, Z. L.; Chan, C. M. *Langmuir* **2003**, *19*, 7417−7422.
(30) Turner-Jones, A.; Bunn, C. W. *Acta Crystallogr.* **1962**, *15*, 105−113.
(31) Jeon, K.; Krishnamoorti, R. *Macromolecules* **2008**, *41*, 7131−7140.